Effect of ortho-substituted aniline on the corrosion protection of aluminum in 2 mol/L H2SO4 solution

NRC Research Press

ARTICLE

Effect of *ortho*-substituted aniline on the corrosion protection of aluminum in 2 mol/L H_2SO_4 solution

Mohamed M. El-Deeb, Hamed M. Alshammari, and Safwat Abdel-Azeim

Abstract: Corrosion protection of aluminum in 2 mol/L H_2SO_4 solution is examined in the presence of *ortho*-substituted aniline derivatives using potentiodynamic polarization and electrochemical impedance spectroscopy measurements. Density function theory (DFT) calculations are performed to investigate the aluminum–electrolyte interface relationship in the absence and presence of both *ortho*-substituted aniline derivatives and sulphate anions, as well as their roles in the protection efficiency at the atomic level. Our results show that *ortho*-aniline derivatives are good inhibitors and that their efficiencies improved as the concentration increased. SEM–EDX analysis is used to confirm the adsorption thermodynamics of the studied compounds on the aluminum surface. The best inhibitory effect is exhibits in the presence of the methyl group in *ortho*-position followed by *ortho*-carboxilic compared to aniline. The adsorption of these compounds on the aluminum surface is well described by Langmuir adsorption isotherm as well as the experimental and the theoretical adosrption energies are in a good agreement. DFT calculations also show that the interaction between the inhibitors and the aluminum surface is mainly electrostatic and depends on the type of the *ortho*-substituted group in addition to the sulphate anions.

Key words: aniline derivatives, aluminum, EIS, SEM–EDX, DFT.

Résumé : Nous avons étudié la protection de l'aluminium contre la corrosion dans une solution de H_2SO_4 à 2 mol/L en présence de dérivés de l'aniline substitués en position *ortho* à l'aide de la polarisation potentiodynamique et de la spectroscopie d'impédance électrochimique. Grâce à des calculs de la théorie de la fonctionnelle de la densité (DFT), nous avons étudié les effets de l'absence ou de la présence de dérivés de l'aniline substitués en position *ortho* ou d'anions sulfate sur l'interface entre l'aluminium et l'électrolyte, ainsi que le rôle à l'échelle atomique que jouent ces composés dans l'efficacité protectrice. Nos résultats montrent que les dérivés d'*ortho*-aniline sont de bons inhibiteurs, et que leur efficacité augmente avec leur concentration. Nous avons utilisé l'analyse MEB–EDX pour corroborer la thermodynamique de l'adsorption sur la surface d'aluminium des composés à l'étude. Le groupe méthyle en position *ortho* offre le meilleur effet inhibiteur par rapport à l'aniline, suivi par le groupe carboxylate en position *ortho*. L'isotherme d'adsorption de Langmuir décrit bien l'adsorption de ces composés sur la surface d'aluminium, comme en témoigne la concordance entre les énergies d'adsorption expérimentales et théoriques. Les calculs de DFT montrent également que l'interaction entre les inhibiteurs et la surface d'aluminium est essentiellement électrostatique et dépend non seulement de la présence des anions sulfate, mais aussi de la nature du groupe en position *ortho*. [Traduit par la Rédaction]

Mots-clés : dérivés de l'aniline, aluminium, SIE, MEB–EDX, DFT.

Introduction

Aluminum is an attractive material for many important technological applications due to its particular properties, including its low density, good appearance, and corrosion protection. The most extensive and biggest uses of aluminum are in packing, transportation, and electrical transmission. For these reasons, the corrosion protection of aluminum was studied by many investigators. Sulphuric acid solutions are used for pickling and chemical and electrochemical etching of aluminum and its alloys. Thus, it is important to control the aluminum corrosion rate in these solutions using a variety of techniques. The use of chemicals as corrosion inhibitors is one of the most effective ways to protect metals and their alloys against the corrosion process; corrosion protection using inhibitors is mainly based on changing the metal surface morphology, induced by the adsorption of these compounds on its surface and formation of a protective blocking layer. Organic compounds containing hetero-atoms and an aromatic ring are widely used to protect metals against the acidic corrosion as a result of sharing their π- and lone pair of electrons with the vacant orbitals of the metal; therefore, the monomeric and polymeric aromatic amines are considered good corrosion inhibitors.[1–4]

Corrosion protection of QD36 steel in 0.5 mol/L HCl solution using aniline, *p*-toluidine, and *p*-anisidine was investigated.[3] The data shows that the corrosion protection occurred through the adsorption of these compounds on steel substrate and the protection efficiencies were enhanced with increasing inhibitor concentrations in the following order: *p*-anisidine > *p*-toluidine > aniline.

Ayobe et al.[5] studied the influence of aniline, *p*-bromoaniline, *m*-chloroaniline, *o*-chloroaniline, *p*-chloroaniline, and *p*-methylaniline on the inhibition of copper corrosion in 8 mol/L H_3PO_4. They found that the presence of these compounds decreases the corro-

Received 26 September 2016. Accepted 5 February 2017.

M.M. El-Deeb. Chemistry Department, Faculty of Science, Ha'il University, 81451 Hail, P.O. Box 2440, KSA; Chemistry Department, Faculty of Science, Beni-Suef University, 62514 Beni-Suef, Egypt.
H.M. Alshammari. Chemistry Department, Faculty of Science, Ha'il University, 81451 Hail, P.O. Box 2440, KSA.
S. Abdel-Azeim. King Abdullah University of Science and Technology (KAUST), KAUST Catalysis Center (KCC), Thuwal 23955-6900, KSA.
Corresponding author: Mohamed M. El-Deeb (email: eldeebm@yahoo.com).

Fig. 1. Structures of *ortho*-substituted aniline. [Colour online.]

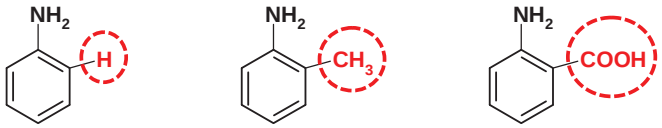

Aniline (An) | **o-toluidine (o-CH_3)** | **o-anthranilic acid (o-COOH)**

Fig. 2. Potentiodynamic polarization plots of aluminum in 2.0 mol/L H_2SO_4 solution in the absence and presence of 300 ppm of An, *o*-COOH, and *o*-CH_3 at 25 °C with scan rate of 10 mV/s. [Colour online.]

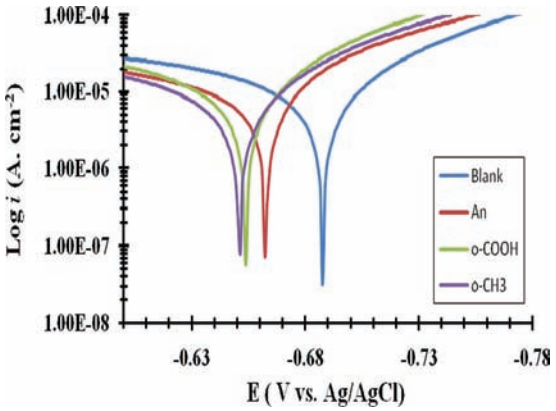

sion rate via the adsorption on the copper surface and the adsorption process obeys Langmuir and Flory–Huggins isotherms.

Khaled and Hackerman[6,7] studied the corrosion inhibition of iron and copper in acidic solutions in the presence of *ortho*-substituted aniline using potentiodynamic polarization and electrochemical impedance techniques. Data showed that all of the investigated compounds had good inhibiting properties and that their efficiency is structure dependent; however, further investigations are necessary to establish an activity – structure efficiency relationship.

Theoretical investigations have been widely used to study the correlation between the molecular structure and the inhibition efficiency.[8,9] Molecular dynamics simulations and quantum calculations were employed to investigated the adsorption mechanism and inhibition efficiency of some Azo-azomethine derivatives on mild steel at different temperatures.[10] The results showed that the abovementioned compounds can be effectively adsorbed on Fe(001) surface via their nitrogen, oxygen, and negatively charged carbon atoms. Wang et al.[11] studied the corrosion inhibition of L-cysteine on AA5052 aluminum alloy in 4 mol/L NaOH solution using experimental and quantum calculations techniques. They found that the carboxylic group, thiol, and amino are mainly active sites absorbed on the surface of aluminum and that the carboxylic group shows the largest absorption ability. Density functional theory (DFT) has become very helpful and popular in studying the metal–electrolyte interface relationship, adsorption properties, and corrosion inhibition mechanism, as well as to analyze the experimental data.[12,13]

The goal of our work is to investigate and explain the corrosion protection of aluminum through studying the aluminum–electrolyte interface relationship in an aggressive sulphuric acid solution in the absence and presence of *ortho*-aniline derivatives (Fig. 1) containing different electronic nature groups (either donating or withdrawing) using electrochemical measurements, surface analysis, and DFT calculations.

Table 1. Electrochemical kinetic parameters and the protection efficiencies of aluminum in 2 mol/L H_2SO_4 solution in the absence (i.e., blank) and presence of different concentrations (*C*) of *ortho*-aniline derivatives (An, *o*-COOH, and *o*-CH_3).

C (ppm)	E_{corr} (mV vs. Ag/AgCl)	I_{corr} (μA/cm²)	B_a (mV/dec)	B_c (mV/dec)	θ	IE (%)
Blank						
—	−699	79.07	84.9	39.12	—	—
An						
10	−697	66.18	84.5	40.6	0.163	16.3
50	−694	56.85	88.2	41.2	0.281	28.1
100	−689	51.24	89.8	37.9	0.352	35.2
150	−683	46.73	90.9	39.6	0.409	40.9
200	−678	41.75	89.5	42.3	0.472	47.2
300	−675	39.85	87.6	41.4	0.496	49.6
***o*-COOH**						
10	−696	57.33	86.3	41.3	0.275	27.5
50	−691	50.53	87.6	43.8	0.361	36.1
100	−685	45.15	87.4	41.5	0.429	42.9
150	−680	34.95	88.7	39.8	0.558	55.8
200	−674	33.60	90.1	40.2	0.575	57.5
300	−666	26.73	89.8	39.7	0.662	66.2
***o*-CH_3**						
10	−694	54.16	84.1	42.2	0.315	31.5
50	−688	41.27	85.2	44.5	0.478	47.8
100	−683	37.48	87.8	38.8	0.526	52.6
150	−679	14.15	81.6	34.7	0.821	82.1
200	−672	10.83	86.5	35.3	0.863	86.3
300	−654	8.22	90.2	36.7	0.896	89.6

Note: B_a and B_c are anodic and cathodic Tafel slopes, respectively.

Fig. 3. Variation of the inhibition efficiencies (IE) vs. inhibitor concentrations (*C*) based on potentiodynamic polarization measurements. [Colour online.]

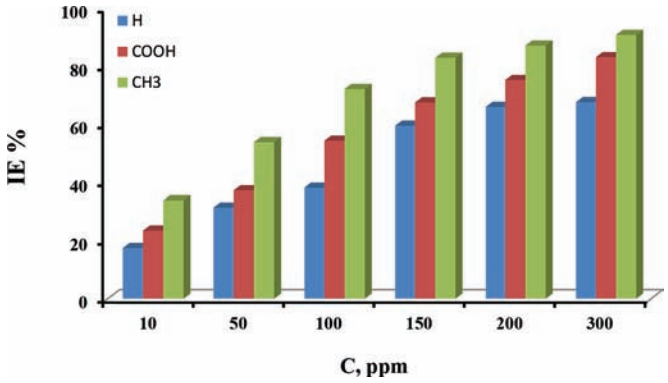

Experimental

Materials

Aniline, *o*-anthranilic acid, *o*-toluidine, and concentrated sulfuric acid are provided from Merck Chemical Co., Germany. All solutions are prepared using deionized water (18.2 μs). Working electrode is made from aluminum rod (area = 1.0 cm^2) with 99.57% purity. Prior to use, it will be polished using emery papers with different grades and then washed and dried.

Electrochemical measurements

Electrochemical measurements are performed on a standard three-compartment glass cell with the aluminum working electrode, Pt counter electrode, and Ag/AgCl reference electrode, to which all potentials are referred. Potentiodynamic current–potential curves are achieved by changing the electrode potential automatically ±100 mV against the E_{OCP}. EIS measurements are carried out using AC signals of amplitude 5 mV peak to peak at the OCP in the

Fig. 4. Nyquist plots of aluminum in 2.0 mol/L H_2SO_4 solution in the (*a*) control sample and in the presence of 300 ppm of (*b*) An, (*c*) *o*-COOH, and (*d*) *o*-CH_3 at E_{OCP}. The inset represents the electrical equivalent circuit model.

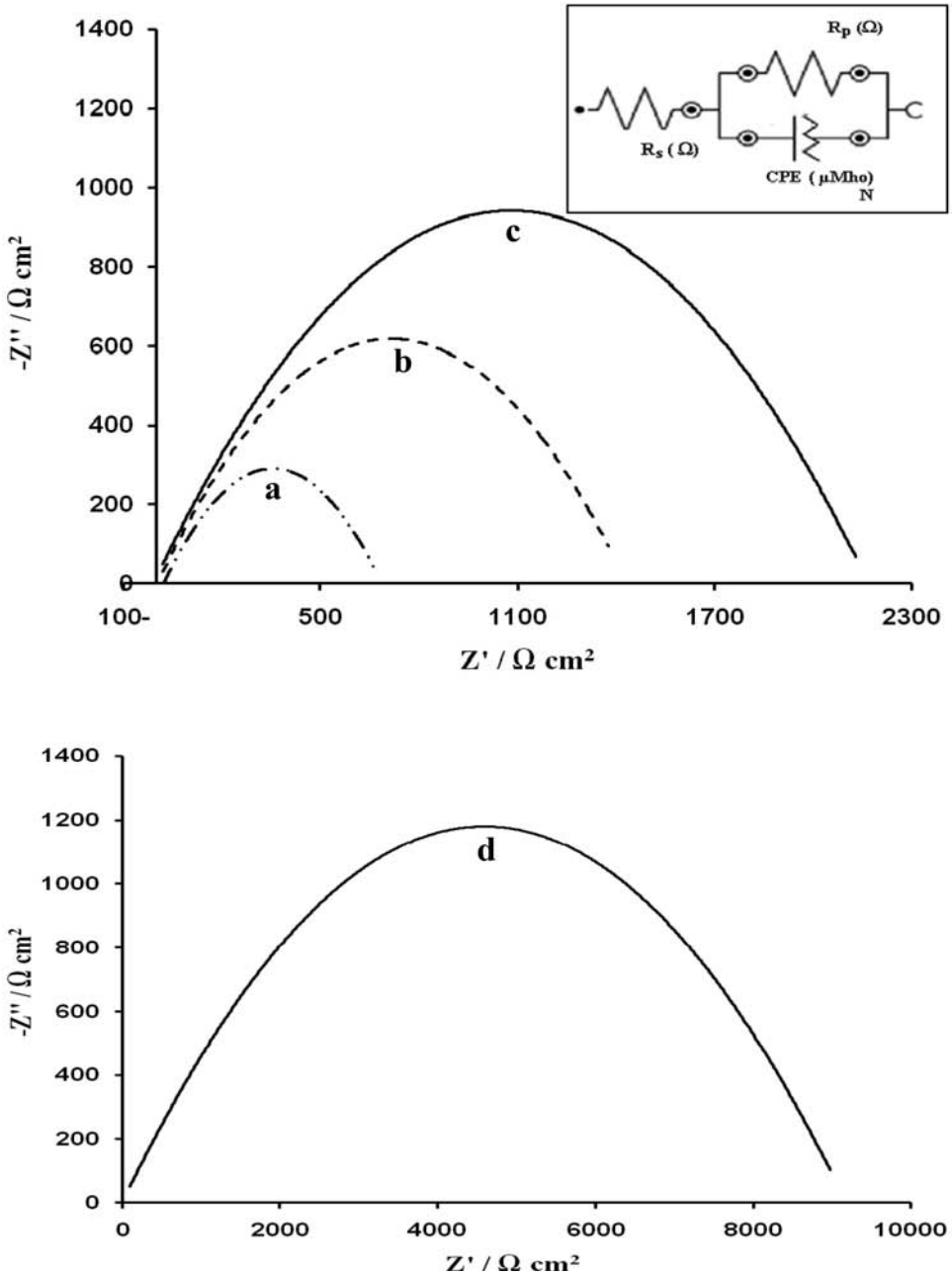

frequency range of 100 kHz to10 MHz. All electrochemical experiments are performed using a potentiostat/galvanostat (Autolab PGSTAT 128N), and NOVA 1.10 software is used for recording and fitting the obtained data.

SEM–EDX analysis

SEM–EDX analysis is carried out using JSM-6510LA (JEOL, Tokyo, Japan). Prior to analysis, aluminum specimens were kept immersed in 2 mol/L H_2SO_4 for 24 h in the absence and presence of 300 ppm of *ortho*-aniline derivatives and then washed and dried.

DFT calculations

All calculations are performed using DFT with the Beck's three-parameter exchange functional along with the Lee–Yang–Parr nonlocal correlation functional (B3LYP)[14–17] and the all-electron triple -ζDef2_TZVP[18,19] basis set using the G09 program.[20] Three complexes are generated by adding three molecules of the *o*-aniline compounds on Al(111) slabs. Due to the computational cost, we have used the Def2_TZVP basis set for all our calculations. The three molecules are adsorbed on clean Al slabs and on a surface covered by a sulphate layer. In all cases, we have fixed Al atoms and optimized the geometry of the *ortho*-aniline derivatives and the sulfate anions.

Results and discussions

Potentiodynamic polarization measurements

Potentiodynamic polarization measurements of aluminum in 2.0 mol/L H_2SO_4 solution are studied by changing the electrode potential automatically ±100 mV against the E_{OCP} in the absence and presence of different concentrations of aniline (An), *ortho*-anthranilic acid (*o*-COOH), and *ortho*-toluidine (*o*-CH_3) at 25 °C with

Fig. 5. Bode plots of aluminum in 2.0 mol/L H_2SO_4 solution in the (*a*) control sample and in the presence of 300 ppm of (*b*) An, (*c*) *o*-COOH, and (*d*) *o*-CH_3 at E_{OCP}.

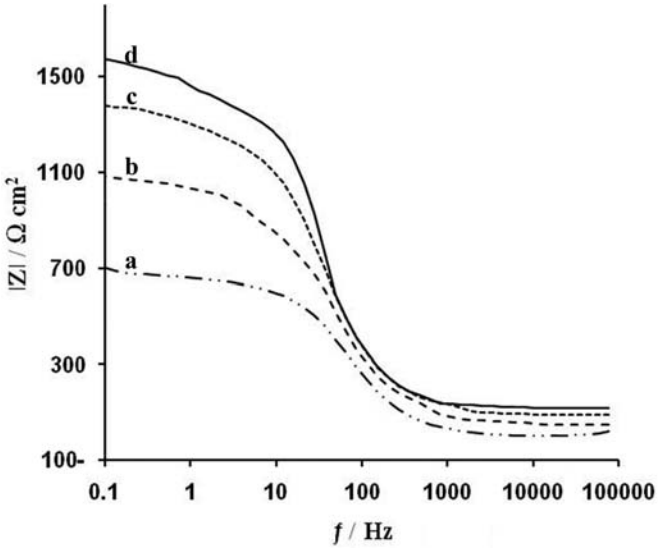

the scan rate of 10 mV/s. The data at 300 ppm are graphically represented in Fig. 2 and the electrochemical parameters and the calculated protection efficiencies[21] are listed in Table 1.

Results show that the higher value of the corrosion current density (79.07 μA/cm²) and the more negative shift in the corrosion potential (–699 mv vs. Ag/AgCl) are in the absence of *ortho*-aniline compounds. This observation can be attributed to the higher rate of both anodic dissolution of aluminum and cathodic reduction of hydrogen. The anodic dissolution of aluminum was explained as a result of the formation of protective Al_2O_3 film on Al surface. Al_2O_3 film can be partially dissolved in the presence of H_2SO_4 solution by the following anodic and cathodic reactions, as previously mentioned:[22,23]

Anodic reactions

(1) $4Al + 3O_2 \rightarrow 2Al_2O_3$

(2) $Al_2O_3 + nH_2O \rightarrow Al_2O_3(H_2O)n$

(3) $Al_2O_3(2H_2O) + 3HSO_4^+ + 3H^+ \rightarrow Al_2[(SO_4)_3(H_2O)_n]_{ads} + 3H_2O$

Cathodic reaction

(4) $2Al_2O_3 + 2H_3O^+ + e^- \rightarrow 2Al_2O_3(H_2O) + H_2\uparrow$

Figure 2 and Table 1 indicate that the addition of *ortho*-aniline derivatives to aluminum in 2.0 mol/L H_2SO_4 reduces the corrosion current densities (I_{corr}) and shifts the corrosion potential (E_{corr}) to more positive values for all of the investigated compounds. The maximum inhibition efficiency (89.6%) is observed at 300 ppm from *o*-toluidine. Generally, it may be concluded from the above results and Fig. 3 that increasing the concentrations of *ortho*-aniline derivatives increases the aluminum surface coverage and, consequently, the inhibition efficiencies. As a result, the adsorption of these compounds on the aluminum surface blocks the active sites for the metal dissolution and the hydrogen evolution.[24] Thus, the addition of these compounds mainly inhibits the partial anodic dissolution of aluminum and also retards the partial cathodic reduction of hydrogen ions. These results reveal that these compounds act as a mixed-type inhibitor and that the inhibition efficiency is in the following order: An < *o*-COOH < *o*-CH_3.

Table 2. Electrochemical parameters and inhibition efficiency of aluminum in 2 mol/L H_2SO_4 solution based on EIS measurements in the absence (i.e., blank) and presence of different concentrations (*C*) of *ortho*-aniline derivatives (An, *o*-COOH, and *o*-CH_3).

C (ppm)	R_s (Ω)	R_p (Ω)	CPE (μMho)	*N*	θ	IE (%)
Blank						
—	0.92	665	9.14	0.899	—	—
An						
10	1.15	818	8.93	0.921	0.187	18.7
50	1.26	941	8.81	0.918	0.293	29.3
100	1.32	1050	8.67	0.905	0.367	36.7
150	1.44	1169	8.42	0.904	0.431	43.1
200	1.67	1301	8.37	0.901	0.489	48.9
300	1.73	1374	8.31	0.912	0.516	51.6
***o*-COOH**						
10	1.21	925	8.80	0.99	0.281	28.1
50	1.37	1062	8.61	0.902	0.374	37.4
100	1.51	1250	8.56	0.907	0.468	46.8
150	1.82	1580	8.11	0.908	0.579	57.9
200	1.91	1714	7.95	0.920	0.612	61.2
300	1.96	2131	7.89	0.915	0.688	68.8
***o*-CH_3**						
10	1.42	1011	8.72	0.901	0.342	34.2
50	1.66	1317	8.39	0.902	0.495	49.5
100	1.78	1481	8.25	0.906	0.551	55.1
150	2.13	4080	7.71	0.908	0.837	83.7
200	2.31	5991	7.68	0.904	0.889	88.9
300	2.48	8986	7.43	0.919	0.926	92.6

Note: R_s and R_p represent the solution resistance and polarization resistance (charge transfer resistance in simple circuit).[36] CPE is the constant phase element corresponding to the double layer capacitance, which was used in the circuit to obtain a better fit in the case of corrosion protection,[37–38] as the metal–solution interface does not behave as an ideal capacitor.[39] *N* is the phase shift related to the inhomogeneities of the double layer[40] associated with the corrosion process.

Fig. 6. Variation of the inhibition efficiencies (IE) vs. inhibitor concentrations (*C*) based on EIS measurements. [Colour online.]

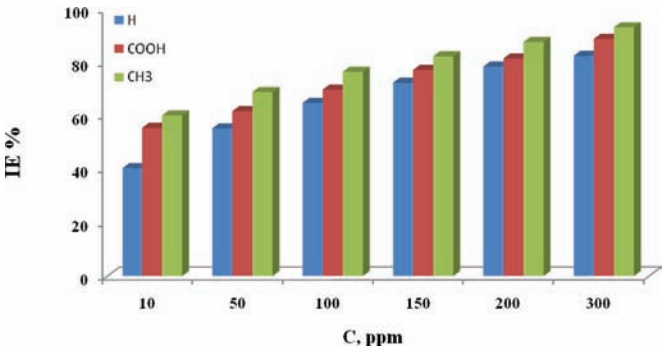

Impedance measurements

EIS is one of the best techniques for analyzing the properties of the metal–electrolyte interface relationship during the corrosion process.[25–28] Nyquist plots of aluminum in 2.0 mol/L H_2SO_4 solution in the absence and presence of different concentrations of *ortho*-aniline derivatives at E_{OCP} are performed over the frequency range of 100 kHz to 10 MHz. The data are graphically represented in case of 300 ppm in Fig. 4. Data shows the presence of one semicircular capacitive loop in the absence and the presence of *ortho*-aniline derivatives that may be correlated to the charge–transfer reaction at the metal–electrolyte interface during the corrosion process.[29–31] The diameter of this capacitive loop increases without any change in the shapes of the Nyquist plot in the presence of *ortho*-aniline derivatives, suggesting the corrosion

Fig. 7. SEM images of the aluminum surface in the control sample and in the presence of 300 ppm of An, *o*-COOH, and *o*-CH_3 at 25 °C after immersion in 2.0 mol/L H_2SO_4 solution for 24 h.

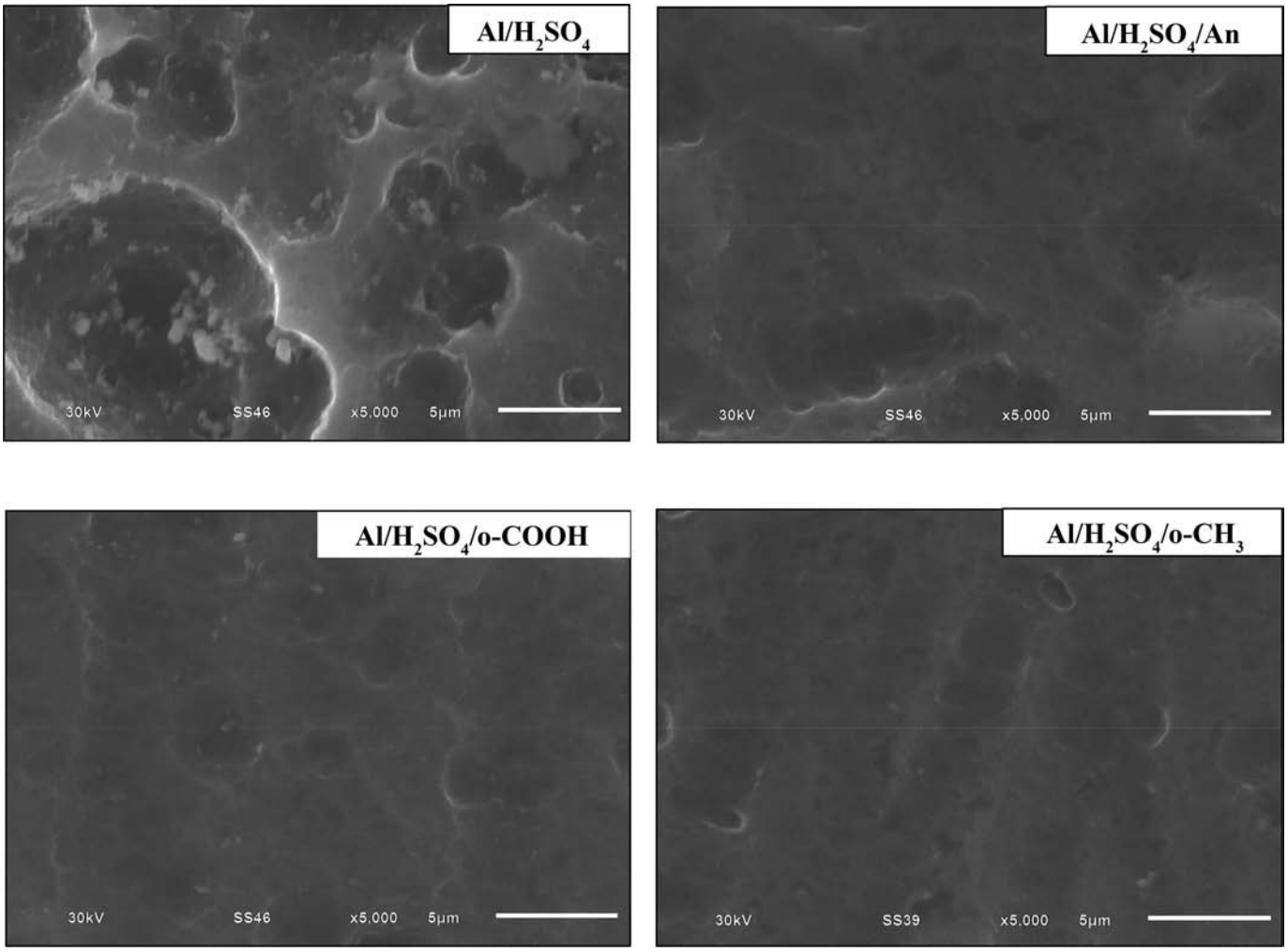

mechanism in the absence and presence of the studied compounds is not changed. The increase in the diameter of capacitive loop that is equivalent to the charge transfer resistance (R_{ct}) can be illustrated as a result of the adsorption of the *ortho*-aniline derivatives on the aluminum surface and acts as a barrier to decrease the rate of aluminum ions transfer and protect it from anodic dissolution in addition to retards the hydrogen evolution process.[32,33] This finding indicates the corrosion resistance of aluminum has been enhanced and the increase in the capacitive loop diameter follows the following order: An < *o*-COOH < *o*-CH_3. The characteristic Nequest shape in Fig. 4 suggests the simple R, C equivalent circuit model with parallel combination of charge transfer resistance (R_{ct}) and double layer capacitance (C_{dl}) due to charge transfer reaction.[34]

Figure 5 illustrates the Bode plots of aluminum in 2.0 mol/L H_2SO_4 solution in the absence and presence of 300 ppm of *ortho*-aniline derivatives. From the figure, it is clear that the presence of one phase for single charge transfer process during aluminum dissolution. The area under the curves in the presence of the studied *ortho*-aniline derivatives is higher than that in the absence of these compounds as a result of the adsorption of these compounds on the aluminum surface that enhances the aluminum surface coverage.

The experimental data recorded by NOVA 1.10 software are fitted to a electrochemical equivalent circuit based on the Boukamp model,[35] and its model is represented in the inset of Fig. 4. The electrochemical parameters derived from the equivalent circuit for aluminum in 2.0 mol/L H_2SO_4 solution in the absence and presence of different concentrations of *ortho*-aniline derivatives are listed in Table 2

Data shows that the structure of the metal–solution interface changes in the presence of these compounds, where R_p values increase with the increasing concentrations of all studied compounds as a consequence of the adsorbed protective layer on the aluminum surface, which makes a charge transfer barrier.[29,30] Interestingly, constant phase element (CPE) values decrease with the increasing concentrations of all studied compounds. This decrease in CPE can be attributed to a replacement of a water molecule by the insulating adsorbed *ortho*-aniline derivatives at the aluminum–electrolyte interface, leading to a decrease in local dielectric constant and (or) an increase the thickness of the barrier layer according to the Helmholtz equation.[41] Therefore, the charge transfer reaction is decreased and the corrosion protection is enhanced. The values of *N* ranged from 0.89 to 0.91, which support the idea that aluminum in the absence and presence of *ortho*-aniline derivatives does not behave as a perfect capacitor.[36] So this finding confirms the replacement of C_{dl} by CPE, as mentioned before.

Figure 6 represents the variation of inhibitor concentrations with the protection efficiency (*P*, %) values calculated from EIS measurements from the following equation:[42]

Table 3. Elemental composition of aluminum in the absence and presence of 300 ppm of *ortho*-aniline derivatives measured by SEM–EDX.

	Composition (mass %)		
Sample	Al	O	C
Al/H_2SO_4	52.93	47.07	—
Al/H_2SO_4/An	86.64	6.58	6.78
Al/H_2SO_4/*o*-COOH	85.15	4.72	10.12
Al/H_2SO_4/*o*-CH_3	46.78	41.61	11.61

$$P_{EIS} = \left(1 - \frac{R_p^{o}}{R_p}\right) \times 100 \quad (5)$$

where R_p^o and R_p are the polarization resistance calculated from EIS measurements for uninhibited and inhibited solutions, respectively. The data clearly show that the values of *P* increase with increasing concentrations for all inhibitors and reach a maximum protection at 300 ppm. The protection efficiency for the studied *ortho*-aniline derivatives increase in the following order: An < *o*-COOH < *o*-CH_3. This order is in a good agreement with other results calculated from the potentiodynamic polarization measurements. Therefore, it can be concluded from the above results that the adsorped *ortho*-aniline derivatives on an aluminum surface change the structure of the metal–solution interface and enhances the corrosion protection of aluminum in sulphuric acid solution.

Surface morphology

SEM images and the elemental composition obtained from the SEM–EDX analysis of aluminum surface in the absence and presence of 300 ppm of An, *o*-COOH, and *o*-CH_3 at 25 °C after immersion in 2.0 mol/L H_2SO_4 solution for 24 h are given in Fig. 7 and Table 3. The obtained data clearly shows the presence of only characteristic pores of Al_2O_3 (corrosion product) in the absence of the *ortho*-aniline compounds. However, the smoother, less corroded surface and the characteristic peak for C appear in the presence of these compounds. This finding indicates that the adsorption of the *ortho*-aniline compounds on aluminum surface and protect the surface from aggressive attack by H_2SO_4 solution.[13]

Adsorption isotherms

The adsorption isotherms can provide significant information about the interaction between *ortho*-aniline compounds and the aluminum surface that can be classified into chemisorption or physisorption depending on the chemical structure of inhibitors and the charges distributed over both inhibitors and metal. The Langmuir adsorption isotherm is tested with the experimental data obtained from the EIS measurements at 25 °C. Figure 8 represents the linear relationship between (C_{inh}/θ) and (C_{inh}) for *ortho*-aniline compounds indicating that the corrosion protection of aluminum by *ortho*-aniline compounds follows the following Langmuir adsorption isotherm[43] and the adsorption occurs in the metal–solution interface:

$$C_{inh}/\theta = (1/K_{ads}) + C_{inh} \quad (6)$$

where K_{ads} is the equilibrium constant for the adsorption–desorption process, C_{inh} is the inhibitor concentration in the solution, and θ (*P*/100) is the surface coverage calculated from EIS measurements at 25 °C. The values of the standard free energy of the adsorption (ΔG^o_{ads}) are obtained using the following equation,[44] and the calculated values of K_{ads} and ΔG^o_{ads} are tabulated in Table 4:

Fig. 8. Langmuir adsorption isotherm based on EIS measurements. [Colour online.]

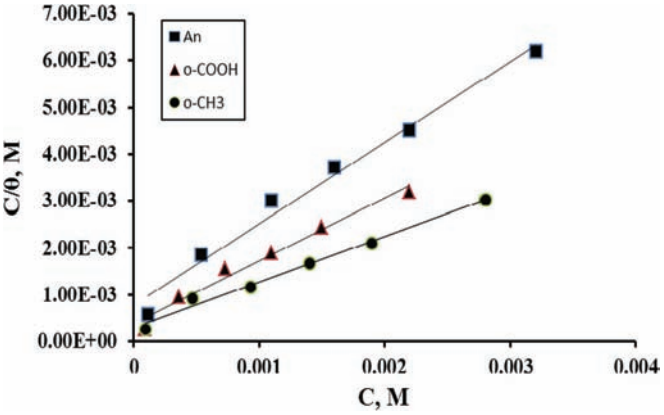

Table 4. Thermodynamic parameters of the adsorption process based on the Langmuir adsorption isotherm.

Inhibitor	K_{ads}, $(mol/L)^{-1}$	ΔG^o_{ads}, kJ/mol
An	1.25×10^3	–27.6
o-COOH	2.5×10^3	–29.3
o-CH_3	3.3×10^3	–30.1

$$\Delta G^o_{ads} = -RT(\ln 55.5 K_{ads}) \quad (7)$$

where *R* is the universal gas constant, *T* is the absolute temperature, and the value 55.5 is the concentration of water in the solution. Data from Table 4 reveal that the adsorption type of *ortho*-aniline compounds on aluminum surface is physisorption. This is a result of the electrostatic interaction between the charged molecules and the charged metal surface that can be characterized by the value of ΔG^o_{ads} at approximately –20 kJ/mol. Also, the higher value of K_{ads} and more negative value of ΔG^o_{ads} in the case of *o*-CH_3 as listed in Table 4 suggests the strong and spontaneous adsorption of this compound on an aluminum surface, which results in a higher protection efficiency compared with *o*-COOH and An.

DFT calculations

DFT calculations are performed to examine the aluminum–electrolyte relationship in the absence and presence of both *ortho*-substituted aniline derivatives and sulphate anions and their effect on the protection efficiency of the anodic dissolution of aluminum in H_2SO_4 solution. A simplified model of Al(111) slabs with three molecules from the studied *ortho*-aniline derivatives (An, *o*-COOH, and *o*-CH_3) adsorbed on its surface is used to take into account the inhibitor–inhibitor interaction. The optimized structures of the three compounds indicate that the interaction between the aluminum surface and the three *ortho*-substituted aniline derivatives depend on the type of the substituents.

The binding energies of the adsorbed molecules (An, *o*-COOH, and *o*-CH_3) are calculated as the energy difference between the complex, the slab, and the isolated molecules. On the clean Al slab (Figs. 9A–9C), the interaction between the *ortho*-aniline derivatives and the aluminum surface is weak, and the values of the binding energies are 0.63, –0.22, and –1.50 kcal/mol for *o*-CH_3, An, and *o*-COOH, respectively. The interaction is mainly electrostatic and the *o*-COOH displays the strongest interaction as a result of the accumulated negative charge from the COOH group while CH_3 (donating group) in the *ortho*-position accumulates positive charge, thus enhancing the repulsion with the Al slab. In both aniline and *o*-toluidine, the compounds are adsorbed in a well-defined layer on

Fig. 9. Adsorption layer of An, *o*-COOH, and *o*-CH_3 on a clean surface (A, B, and C) and on a slab of Al covered by a layer of sulfate (D, E, and F), respectively. [Colour online.]

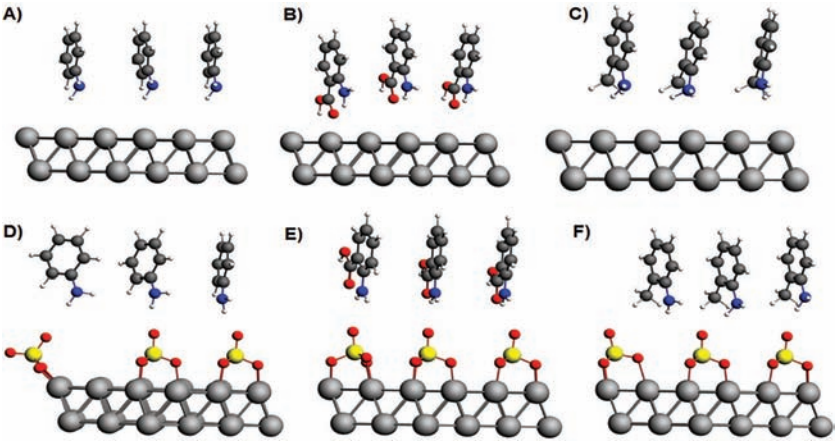

the Al slab, whereas in the case of the anthranilic acid, the adsorbed layer is slightly distorted (Fig. 9).

To examine the effect of the sulfate anions on the interaction of these three compounds with the Al surface, we have adopted another model in which the Al surface is covered by a sulfate layer. The interaction with the Al slab covered by a layer of sulfate is much stronger, and this is evidenced by the much lower interaction energies compared with the clean surface (the binding energy became –16.68, –15.30, and –14.22 kcal/mol for *o*-CH3, An, and *o*-COOH, respectively).[45–47]

The presence of the CH_3 group (donating group) in *o*-toluidine strengthens the interaction with the sulfate layer as it accumulates positive charge and, consequently, strengthens the interaction with the negatively charged sulfate groups adsorbed on the Al surface. However, the presence of the COOH group (withdrawing group) is harmful for the adsorption, as it increases the electrostatic repulsion with the sulfate layer.

The experimental adsorption energies of *o*-CH_3, *o*-COOH, and An are –30.1, –29.3, and –27.6 kJ/mol and show good agreement with the DFT-calculated adsorption energies (–16.68, –15.30, and –14.22 kcal/mol for *o*-CH_3, *o*-COOH, and An, respectively). The agreement between the experimental and the DFT-calculated adsorption energies of *ortho*-aniline derivatives with the Al surface covered with a layer of sulfate supports the hypothesis that the corrosion protection of aluminum in 2 mol/L H_2SO_4 solution occurs through the adsorption of these compounds on the aluminum covered with the sulphate anions.

The calculated band gap of HOMO–LUMO in case of the Al slab covered with sulfate layer shows that *o*-CH_3 (559.4 mev) is the most efficient compound, as it exhibits the highest band gap, whereas aniline is the least efficient compound with a band gap of 230.0 mev and *o*-COOH exhibits an intermediate efficiency with a band gap of 243.0 mev. However, in case of the clean surface, the band gap does not show any significant difference between the *ortho*-aniline derivatives (452.9, 449.6, and 452.7 mev for An, *o*-COOH, and *o*-CH_3, respectively). It is worth noting that the band gap trend and the adsorption energies in the case of the clean surface do not show any correlation with the experimental data. However, the band-gap trend of the three compounds and the adsorption energies in the case of Al surface covered by sulfate layer agree well with the experimental measurements. These results indicate that *o*-CH_3 is the most efficient compound to protect the Al surface in H_2SO_4 solution.

Conclusion

1. Corrosion protection of aluminum in 2 mol/L H_2SO_4 solution is investigated using *ortho*-aniline derivatives at 25 °C by electrochemical techniques, surface analysis, and DFT calculations.
2. Potentiodynamic polarization and EIS measurements showed that all *ortho*-aniline derivatives are good inhibitors and that the protection efficiency increases with increasing their concentrations, giving 92.6% in case of 300 ppm of *o*-toluidine.
3. The adsorption of *ortho*-aniline derivatives followed the Langmuir adsorption isotherm.
4. SEM–EDX analysis showed a smoother, less corroded surface and the characteristic peak for carbon in the presence of *ortho*-aniline derivatives, whereas the characteristic pores of Al_2O_3 appeared in plank solution.
5. DFT calculations clarified that the interaction between the *ortho*-aniline derivatives and the clean aluminum surface is mainly electrostatic. This interaction became much stronger when the Al surface was covered by a sulfate layer. The strength of this interaction depends on the type of substituents in the *ortho* position.
6. The adsorbed *ortho*-aniline derivatives on aluminum surface change the Al–electrolyte interface.

References

(1) Vashi, R. T.; Naik, D. *Int. J. ChemTech Res.* **2011**, *3*, 864.
(2) El-Deeb, M. M.; Mohamed, S. M. *J. Appl. Polym. Sci.* **2011**, *122*, 3030. doi:10.1002/app.34115.
(3) El-Haddad, M. N.; Fouda, A. E. S. *Prot. Met. Phys. Chem. Surf.* **2013**, *49*, 753. doi:10.1134/S2070205113060191.
(4) Sayyah, S. M.; Abd El-Rehim, S. S.; El-Deeb, M. M.; Mohamed, S. M. *Egypt. J. Chem.* **2012**, *55*, 583.
(5) Ayobe, E. A.; Abaza, S. F.; Seleim, S. M.; Ahmed, A. M. *Indian J. Chem. Technol.* **2012**, *19*, 322.
(6) Khaled, K. F.; Hackerman, N. *Electrochim. Acta* **2003**, *48*, 2715. doi:10.1016/S0013-4686(03)00318-9.
(7) Khaled, K. F.; Hackerman, N. *Electrochim. Acta* **2004**, *49*, 485. doi:10.1016/j.electacta.2003.09.005.
(8) Sayyah, S. M.; El-Deeb, M. M.; Abd El-Rehim, S. S.; Ghanem, R. A.; Mohamed, S. M. *Port. Electrochim. Acta* **2014**, *32*, 417. doi:10.4152/pea.201406417.
(9) Awad, M. K.; Metwally, M. S.; Soliman, S. A.; El-Zomrawy, A. A.; Bedair, M. A. *J. Ind. Eng. Chem.* **2014**, *20*, 796. doi:10.1016/j.jiec.2013.06.009.
(10) Shokry, H. *J. Mol. Struct.* **2014**, *1060*, 80. doi:10.1016/j.molstruc.2013.12.030.
(11) Wang, D.; Gao, L.; Zhang, D.; Yang, D.; Wang, H.; Lin, T. *Mater. Chem. Phys.* **2016**, *169*, 142. doi:10.1016/j.matchemphys.2015.11.041.
(12) Zarrouk, A.; Zarrok, H.; Salghi, R.; Hammouti, B.; Al-Deyab, S. S.; Touzani, R.; Bouachrine, M.; Warad, I.; Hadda, T. B. *Int. J. Electrochem. Sci.* **2012**, *7*, 6353.
(13) Wang, D.; Yang, D.; Zhang, D.; Li, K.; Gao, L.; Lin, T. *Appl. Surf. Sci.* **2015**, *357*, 2176. doi:10.1016/j.apsusc.2015.09.206.
(14) Becke, A. D. *J. Chem. Phys.* **1993**, *98*, 5648. doi:10.1063/1.464913.
(15) Lee, C.; Yang, W.; Parr, R. G. *Phys. Rev. B* **1988**, *37*, 785. doi:10.1103/PhysRevB.37.785.
(16) Vosko, S. H.; Wilk, L.; Nusair, M. *Can. J. Phys.* **1980**, *58*, 1200. doi:10.1139/p80-159.

(17) Stephens, P. J.; Devlin, F. J.; Chabalowski, C. F.; Frisch, M. J. *J. Phys. Chem.* **1994**, *98*, 11623. doi:10.1021/j100096a001.
(18) Weigend, F.; Ahlrichs, R. *Phys. Chem. Chem. Phys.* **2005**, *7*, 3297. doi:10.1039/b508541a.
(19) Weigend, F. *Phys. Chem. Chem. Phys.* **2006**, *8*, 1057. doi:10.1039/b515623h.
(20) Frisch, M. J.; Trucks, G. W.; Schlegel, H. B.; Scuseria, G. E.; Robb, M. A.; Cheeseman, J. R.; Scalmani, G.; Barone, V.; Mennucci, B.; Petersson, G. A.; Nakatsuji, H.; Caricato, M.; Li, X.; Hratchian, H. P.; Izmaylov, A. F.; Bloino, J.; Zheng, G.; Sonnenberg, J. L.; Hada, M.; Ehara, M.; Toyota, K.; Fukuda, R.; Hasegawa, J.; Ishida, M.; Nakajima, T.; Honda, Y.; Kitao, O.; Nakai, H.; Vreven, T.; Montgomery, J. A., Jr.; Peralta, J. E.; Ogliaro, F.; Bearpark, M.; Heyd, J. J.; Brothers, E.; Kudin, K. N.; Staroverov, V. N.; Kobayashi, R.; Normand, J.; Raghavachari, K.; Rendell, A.; Burant, J. C.; Iyengar, S. S.; Tomasi, J.; Cossi, M.; Rega, N.; Millam, J. M.; Klene, M.; Knox, J. E.; Cross, J. B.; Bakken, V.; Adamo, C.; Jaramillo, J.; Gomperts, R.; Stratmann, R. E.; Yazyev, O.; Austin, A. J.; Cammi, R.; Pomelli, C.; Ochterski, J. W.; Martin, R. L.; Morokuma, K.; Zakrzewski, V. G.; Voth, G. A.; Salvador, P.; Dannenberg, J. J.; Dapprich, S.; Daniels, A. D.; Farkas, Ö.; Foresman, J. B.; Ortiz, J. V.; Cioslowski, J.; Fox, D. J. *Gaussian 09, Revision D.01*; Gaussian: Wallingford, CT, 2009.
(21) El-Deeb, M. M.; Sayyah, S. M.; Abd El-Rehim, S. S.; Mohamed, S. M. *Arabian J. Chem.* **2015**, *8*, 527. doi:10.1016/j.arabjc.2013.09.018.
(22) Arellanes-Lozada, P.; Olivares-Xometl, O.; Guzmán-Lucero, D.; Likhanova, N.; Domínguez-Aguilar, M.; Lijanova, I.; Arce-Estrada, E. *Materials* **2014**, *7*, 5711. doi:10.3390/ma7085711.
(23) El-Etre, A. Y. *Corros. Sci.* **2003**, *45*, 2485. doi:10.1016/S0010-938X(03)00066-0.
(24) Ehsani, A.; Ahmadi, M.; Ghanbari, M. *Adv. Anal. Chem.* **2015**, *5*, 19.
(25) Mansfeld, F.; Kendig, M. W.; Tsai, S. *Corrosion* **1982**, *38*, 478. doi:10.5006/1.3577363.
(26) Mansfeld, F. *J. Appl. Electrochem.* **1995**, *25*, 187. doi:10.1007/BF00262955.
(27) Ehsani, A.; Babaei, F.; Nasrollahzadeh, M. *Appl. Surf. Sci.* **2013**, *283*, 1060. doi:10.1016/j.apsusc.2013.07.067.
(28) Abd, El; Rehim, S. S.; Sayyah, S. M.; El-Deeb, M. M.; Kamal, S. M.; Azooz, R. E. *Int. J. Ind. Chem.* **2016**, *7*, 39. doi:10.1007/s40090-015-0065-5.
(29) Khaled, K. F.; Atta, A. A.; Abdel-Shafi, N. S. *J. Mater. Environ. Sci.* **2014**, *5*, 831.
(30) El-Haddad, M. N.; Fouda, A. S. *J. Mol. Liq.* **2015**, *209*, 480. doi:10.1016/j.molliq.2015.06.005.
(31) Yıldız, R. *Corros. Sci.* **2015**, *90*, 544. doi:10.1016/j.corsci.2014.10.047.
(32) Döner, A.; Kardaş, G. *Corros. Sci.* **2011**, *53*, 4223. doi:10.1016/j.corsci.2011.08.032.
(33) Solmaz, R.; Altunbaş, E.; Kardaş, G. *Mater. Chem. Phys.* **2011**, *125*, 796. doi:10.1016/j.matchemphys.2010.09.056.
(34) Walter, G. W. *Corros. Sci.* **1986**, *26*, 681. doi:10.1016/0010-938X(86)90033-8.
(35) Boukamp, B. A. *Solid State Ionics* **1986**, *20*, 31. doi:10.1016/0167-2738(86)90031-7.
(36) Tammam, R. H.; Fekry, A. M.; Saleh, M. M. *Int. J. Electrochem. Sci.* **2016**, *11*, 1310.
(37) Fekry, A. M. *Electrochim. Acta* **2009**, *54*, 3480. doi:10.1016/j.electacta.2008.12.060.
(38) Macdonald, D. D. *Electrochim. Acta* **2006**, *51*, 1376. doi:10.1016/j.electacta.2005.02.107.
(39) Behpour, M.; Ghoreishi, S. M.; Soltani, N.; Salavati-Niasari, M. *Corros. Sci.* **2009**, *51*, 1073. doi:10.1016/j.corsci.2009.02.011.
(40) Özcan, M.; Karadağ, F.; Dehri, İ. *Colloids Surf., A* **2008**, *316*, 55. doi:10.1016/j.colsurfa.2007.08.023.
(41) Hassan, H. H. *Electrochim. Acta* **2006**, *51*, 5966. doi:10.1016/j.electacta.2006.03.065.
(42) Ehsani, A.; Nasrollahzadeh, M.; Mahjani, M. G.; Moshrefi, R.; Mostaanzadeh, H. *J. Ind. Eng. Chem.* **2014**, *20*, 4363. doi:10.1016/j.jiec.2014.01.045.
(43) Abd, El; Rehim, S. S.; Sayyah, S. M.; El-Deeb, M. M.; Kamal, S. M.; Azooz, R. E. *Mater. Chem. Phys.* **2010**, *123*, 20. doi:10.1016/j.matchemphys.2010.02.069.
(44) Musa, A. Y.; Jalgham, R. T. T.; Mohamad, A. B. *Corros. Sci.* **2012**, *56*, 176. doi:10.1016/j.corsci.2011.12.005.
(45) Ren, X.; Xu, S.; Chen, S.; Chen, N.; Zhang, S. *RSC Adv.* **2015**, *5*, 101693. doi:10.1039/C5RA21050J.
(46) Fouda, A. S.; El-Haddad, M. N. *Int. J. Chem. Mater. Sci.* **2015**, *3*, 33.
(47) Chen, S.; Kar, T. *Int. J. Electrochem. Sci.* **2012**, *7*, 6265.